

DFT and experimental studies on structure and spectroscopic parameters of 3,6-diiodo-9-ethyl-9H-carbazole

Klaudia Radula-Janik¹ · Teobald Kupka¹ · Krzysztof Ejsmont¹ · Zdzisław Daszkiewicz¹ · Stephan P. A. Sauer²

Received: 17 November 2015 / Accepted: 19 November 2015 / Published online: 8 December 2015
© The Author(s) 2015. This article is published with open access at Springerlink.com

Abstract The first report on crystal and molecular structure of 3,6-diiodo-9-ethyl-9H-carbazole is presented. Experimental room-temperature X-ray and ¹³C chemical shift studies were supported by advanced theoretical calculations using density functional theory. The ¹³C nuclear magnetic shieldings were predicted at the non-relativistic and relativistic level of theory using the zeroth-order regular approximation. Theoretical relativistic calculations of chemical shifts of carbons C3 and C6, directly bonded to iodine atoms, produced a reasonable agreement with experiment (initial deviation from experiment of 44.3 dropped to 4.25 ppm). The changes in ring aromatic character were estimated via a simple harmonic oscillator model of aromaticity and nucleus-independent chemical shift index calculations. A good linear correlation between experimental and theoretically predicted structural and NMR parameters was observed.

Keywords 3,6-diiodo-9-ethyl-9H-carbazole · X-ray structure · ¹³C NMR spectra · ZORA GIAO NMR calculations

Introduction

Carbazoles are very interesting heterocyclic derivatives of the aromatic hydrocarbon phenanthrene. Since decades they are used in industrial applications of polyvinylcarbazole (PVCZ) in electrophotographic materials [1]. In addition, carbazole derivatives are precursors of materials used in electronics and photonics [2–5]. This field is particularly important as a remedy for the emerging world energy crisis due to population growth and technological development of rapidly growing countries in Asia, e.g., China and India. The most widely studied materials are 3,6-substituted and 2,7-substituted carbazole derivatives [6–9]. Carbazole derivatives have very interesting photoconductivity [10] and optical [11] properties. Due to their fluorescent ability, carbazoles are used for the production of light emitting diodes (OLEDs) [12, 13] and sensors [14–17]. For these reasons, there is a constant search for new carbazole derivatives as potential substrates for new materials with promising optoelectronic properties.

Nuclear magnetic resonance (NMR) is a useful method for molecular structure determination [18]. Molecular modeling of NMR parameters is widely used to support assignments of experimental spectra [19–21]. Satisfactory chemical shifts for several different nuclei including ¹³C, ¹⁷O, ¹⁵N and ¹⁹F [19, 22–25] can be obtained by density functional theory calculations in combination with gauge including atomic orbitals (GIAO) [26, 27] and employing the Becke, three-parameter, Lee–Yang–Parr (B3LYP) [27, 28] or BHandHLYP hybrid half-and-half functional [29]. In particular the latter was used to predict accurate NMR parameters. Several reports on NMR studies of the simplest carbazoles are available [30–33]. In most theoretical works, the predicted (non-relativistic) chemical shifts of atoms adjacent to a heavy atom are not accurate due to

Electronic supplementary material The online version of this article (doi:10.1007/s11224-015-0711-8) contains supplementary material, which is available to authorized users.

✉ Teobald Kupka
teobaldk@gmail.com

¹ Faculty of Chemistry, Opole University, 48, Oleska Street, 45-052 Opole, Poland

² Department of Chemistry, University of Copenhagen, Universitetsparken 5, 2100 Copenhagen, Denmark

omitting of relativistic effects in typical GIAO NMR calculations. The heavy nucleus (here iodine) effect can be observed for light nuclei (^1H , ^{13}C , ^{15}N) in the proximity of heavy atoms and it was described by Pyykkö et al. [34] as the heavy-atom-on-light-atom (HALA) effect. Early relativistic calculations of NMR shieldings were reported by Malkin, Ziegler and Autschbach [35–40]. The importance of the HALA effect of mercury on the isotropic shielding of carbon atoms was reported by Wodyński et al. [41]. They obtained significant HALA effects in halogen-substituted compounds, which were well reproduced using the zeroth-order regular approximation with spin–orbit coupling (SO ZORA) [42–44]. This effect could not be recovered by using relativistic effective core potentials (ECP) [45] on the halogen atoms. The work of Wodyński and Pecul [46] described the influence of the presence of a heavy atom on the spin–spin coupling constants between two light nuclei in organometallic compounds and halogen derivatives.

The structural and electronic parameters of carbazoles have been analyzed by means of different aromaticity criteria. This chemical property can be carried out through the use of structurally (HOMA), electronically (PDI—para-delocalization index) and magnetically (NICS) based indices. The work of Poater et al. [47] showed a clear divergence between the structural, electronic and magnetic measures, so it is important to use different aromaticity indices to quantify this property. The structurally based measure is described as an harmonic oscillator model of aromaticity (HOMA) and defined by Kruszewski and Krygowski as [48, 49]:

$$\text{HOMA} = 1 - \frac{\alpha}{n} \sum_{i=1}^n (R_{\text{opt}} - R_i)^2 \quad (1)$$

where n is the number of included bonds with bond lengths R_i , and α is an empirical constant chosen in such a way that $\text{HOMA} = 0$ for a model nonaromatic system, and $\text{HOMA} = 1$ for a system with all bonds equal to an optimal value R_{opt} , assumed to be achieved for fully aromatic systems. The HOMA index has been found to be among the most effective structural indicators of aromaticity [50]. Another aromaticity criterion based on the electron ring current is the widely employed nucleus-independent chemical shift (NICS). This index was proposed by Schleyer et al. [51]. NICS is defined as the negative value of the absolute shielding computed at the ring center or at some other interesting geometrical point above the ring system. In common use are three variants: NICS(0) calculated at the ring plane, NICS(1) calculated 1 Å above the plane and its zz tensor component, NICS(1) $_{zz}$, where the z -axis is normal to the plane. Rings with large negative NICS values are considered to be aromatic, and the more negative the NICS value is, the more aromatic the rings are. The work of Chen et al. [52] shows that NICS calculations

are relatively insensitive to the employed level of theory. On the other hand, NICS indexes are sensitive to the number of π -electrons in the systems. Thus, the 10 π -electron systems show higher NICS values than the 6 π -electron systems [52].

Molecular modeling of structural and spectroscopic parameters has been a relatively inexpensive and fast way leading to practical application of numerous compounds. Surprisingly, no systematic theoretical and experimental studies on structure of diiodo derivatives of carbazoles are available. As part of detailed studies on carbazole, we undertook theoretical characterization of 3,6-diiodo-9-ethyl-9H-carbazole supported by room-temperature X-ray determination of previously unknown crystal structure.

The aim of our study was to determine the structural parameters of diiodocarbazole derivative molecules using DFT calculations with efficient B3LYP hybrid density functional and mixed 6-311++G(3df,2pd) and 6-311++G** basis sets. Moreover, we estimated the changes in ring aromatic character via simple HOMA and NICS calculations. The theoretical structural parameters were additionally supported by crystal structure studies of the corresponding N9-ethyl derivative.

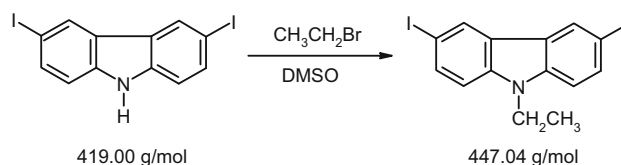
Experimental

Synthesis

3,6-Diiodo-9H-carbazole was obtained according to the procedure described by Chuang et al. [53]. A solution containing 16.7 g (0.1 mol) of 9H-carbazole, 21.6 g (0.13 mol) of KI, 21.4 g (0.1 mol) of KIO_3 , 150 cm^3 of acetic acid and 15 cm^3 of water was heated for 48 h on a water bath at 80 °C. After cooling to the room temperature, the precipitate was filtered off and washed with water, saturated Na_2CO_3 solution and methanol. The crude product was crystallized from toluene. The yield was 25 g of 3,6-diiodo-9H-carbazole (mp. 206–207 °C; Ed. 60 %).

The preparation of 3,6-diiodo-9-ethyl-9H-carbazole is shown in scheme 1.

To the intensively stirred solution of 2 g (4.77 mmol) of 3,6-diiodo-9H-carbazole in DMSO (30 ml) and tetrabutylammonium iodide (0.2 g) was added 50 % aqueous KOH solution (2 ml) and treated dropwise with 1.2 ml



Scheme 1 Synthesis of 3,6-diiodo-9-ethyl-9H-carbazole

(16 mmol) of ethyl bromide in DMSO (10 ml). After 2 h the mixture was poured into water (100 ml). The precipitate was dissolved in methylene chloride (30 ml) and dried with anhydrous MgSO_4 . After evaporation of the solvent, the residue (2.0 g) was crystallized from 30 ml of n-heptane. The yield was 1.9 g of 3,6-diiodo-9-ethyl-9H-carbazole (mp. = 154–155 °C; Ed. 90.0 %).

The crystals suitable for X-ray analysis of 3,6-diiodo-9-ethyl-9H-carbazole were obtained by slow evaporation of a saturated solution in chloroform.

Characterization

The single crystals of 3,6-diiodo-9-ethyl-9H-carbazole were used for data collection at 293(2)K on a four-circle Oxford Diffraction Xcalibur diffractometer equipped with a two-dimensional area CCD detector with the graphite monochromatized $\text{MoK}\alpha$ radiation ($\lambda = 0.71073 \text{ \AA}$) and the ω -scan technique. Integration of the intensities and correction for Lorentz and polarization effects were performed using the CrysAlis RED software [54]. Crystal structures were solved by direct methods and refined by a full-matrix least-squares method on F^2 using the SHELXL-97 program [55]. Complete crystallographic details are available as a supplementary material and have been deposited at the Cambridge Crystallographic Data Centre (CCDC 1051894) CCDC [56]. The ^{13}C NMR spectra in CDCl_3 solution were measured using Bruker Ultrashield 400 MHz NMR spectrometer operating at 100.623 MHz for carbon nuclei at ambient temperature and referenced to benzene and tetramethylsilane (TMS).

Theoretical calculations

The molecular geometry of the isolated molecule was obtained from an unconstrained optimization of all geometrical parameters using the B3LYP functional and a flexible 6-311++G(3df,2pd) basis set for all atoms with the exception of iodine, for which the smaller basis set (6-311G**) was used. No imaginary frequencies were found, which indicated the true energy minimum. These non-relativistic (NR) calculations were carried out using GAUSSIAN 09 [57]. In our previous work [58], we reported on the structural parameters for 9-benzyl-3,6-diiodo-9H-carbazole obtained at the relativistic (R) SO ZORA (B3LYP/DZP/TZP) level of theory. These results were of similar accuracy to the results of the non-relativistic calculations. Besides, it was significantly faster to get non-relativistic results. Next, the non-relativistic geometry has been used for both the relativistic zeroth-order regular approximation Hamiltonian including the spin-orbit coupling term (SO ZORA) [59] and non-relativistic shielding calculations with the half-and-half hybrid BHandHLYP functional and

STO type DZP basis set. All NMR parameters were obtained with Amsterdam density functional (ADF) program [60]. Theoretical chemical shifts (in ppm) were referenced to benzene and tetramethylsilane (TMS) calculated at the same level of theory.

Both HOMA and NICS are non-local parameters (averaged over the total molecular structure) and should be “the same” using NR and R approaches. Thus, in the current study we applied the cheaper non-relativistic approach. HOMA and NICS indexes of aromaticity were calculated at B3LYP/6-311++G(3df,2pd) level of theory using Gaussian 09.

Results and discussion

Crystal structure

The molecular structure of 3,6-diiodo-9-ethyl-9H-carbazole, the atomic numbering and ring labeling schemes are presented in Fig. 1. The packing arrangement in the crystal state is presented in Fig. 2. 3,6-Diiodo-9-ethyl-9H-carbazole crystallizes in the monoclinic space group P2_1 . The bond lengths within carbazole skeleton of this molecule are in a good agreement with the corresponding distances in the unsubstituted carbazole [61]. The ethyl group forms a dihedral angle of 179.86° with the carbazole skeleton. In the crystal structure, the ethyl group (C10–C11–H11A) forms an angle of 86.48° with the C1–C9A ring. The angle between the second ring (C5–C8A) and ethyl group is nearly identical (84.42°). The intermolecular interactions [C(5)–H(5)···I(1)] in the crystal lattice are shown in Fig. 2.

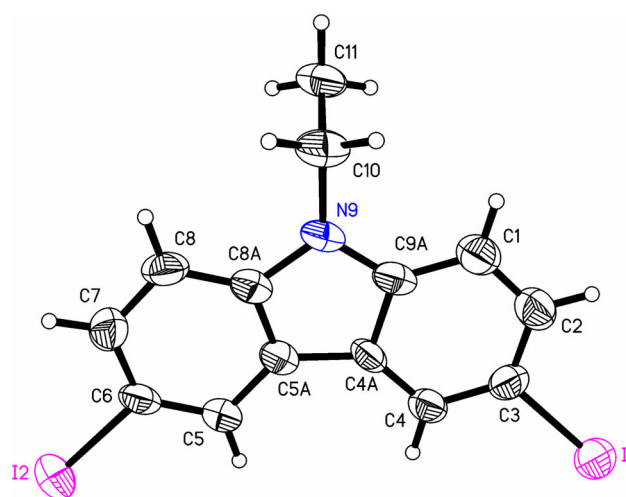


Fig. 1 Molecular structure of 3,6-diiodo-9-ethyl-9H-carbazole, showing the atom numbering scheme and the ring labeling. Displacement ellipsoids are drawn at the 50 % probability level

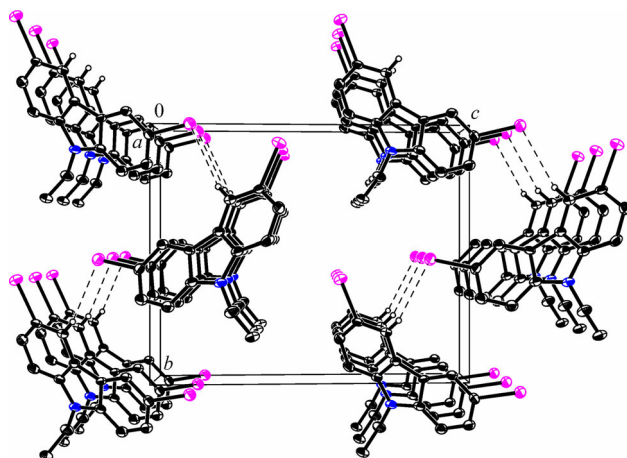


Fig. 2 A packing diagram for 3,6-diiodo-9-ethyl-9H-carbazole, showing the weak C5–H5...I1ⁱ bonds as *dashed lines*. [Symmetry code: $i = -x - 1, y - 0.5, -z$]

The crystal data and refinement parameters are summarized in Table 1. The intermolecular bonds between hydrogen and iodine atoms in neighboring molecules are given in Table 2. Selected bond lengths are given in Table 3. For brevity, all experimental bond distances, bond angles and torsion angles within this compound are given in Tables S1, S2 and S3 in the Supporting Information. The differences between theoretical and experimental C–C bond lengths are in the range of 0.004–0.04 Å. For the C–N bonds the error range is smaller (0.008–0.017 Å). The largest differences were observed for C–I bonds (0.027–0.034 Å). From the data in Table 3 it is apparent that the accuracy of structure calculations is close to experimental errors. In the gas phase the C–I bonds are the same due to symmetry. In the crystal such long-range interactions are very weak and the experimental difference is within the measurement accuracy (0.007 ± 0.008 Å, see Table 3).

All geometric parameters for the newly synthesized diiodocarbazole derivative are in good agreement with values found in the crystal structure of the nonhalogenated 9-ethyl-9H-carbazole [62] and the other halogenated (3,6-diiodo-9H-carbazole) [63] (Table 3). The total root-mean-square (RMS) between our non-relativistic results and X-ray determinate geometry is 0.021 Å.

According to categorization of H bonds by Jeffrey [64], the H...I bond is a moderate, electrostatic bond. The H...A distance is shorter than the sum of the van der Waals radii proposed by Bondi [65] (3.18 Å).

¹³C NMR chemical shift

The ¹³C chemical shifts (experimental and theoretically predicted) of 3,6-diiodo-9-ethyl-9H-carbazole are collected in Table 4. The very large HALA effect of about –44 ppm

Table 1 Crystallographic data for 3,6-diiodo-9-ethyl-9H-carbazole at room temperature

| 3,6-Diiodo-9-ethyl-9H-carbazole | |
|---|---|
| Chemical formula | C ₁₉ H ₁₃ I ₂ N |
| M _r | 447.04 |
| Cell setting, space group | Monoclinic, P2 ₁ |
| Temperature (K) | 293(2) |
| <i>a</i> (Å), <i>b</i> (Å), <i>c</i> (Å) | 4.4223(4), 11.1936(9), 13.8273(12) |
| β (°) | 94.081(8) |
| <i>V</i> (Å ³) | 682.74(10) |
| <i>Z</i> | 2 |
| <i>D_x</i> (mg m ⁻³) | 2.175 |
| Radiation type | MoK α |
| μ (mm ⁻¹) | 4.584 |
| Crystal size (mm) | 0.20 × 0.18 × 0.16 |
| No. of measured, independent and observed reflections | 4268/2401/2294 |
| <i>R</i> _{int} | 0.0259 |
| ($\sin \theta / \lambda$) _{max} (Å ⁻¹) | 0.595 |
| <i>R</i> [<i>F</i> ² > 2 σ (<i>F</i> ²)], <i>wR</i> (<i>F</i> ²), <i>S</i> | 0.0448, 0.1106, 1.042 |
| No. of reflections | 2401 |
| No. of parameters | 154 |
| No. of restraints | 1 |
| H-atom treatment | All H atoms were generated in idealized positions, no ref. |
| Weighting scheme | $w = 1 / [\sigma^2(F_o^2) + (0.0895P)^2 + 0.0000P]$ where $P = (F_o^2 + 2F_c^2) / 3$ |
| $\Delta\rho_{max}$, $\Delta\rho_{min}$ (e Å ⁻³) | 1.918 –1.057 |

Table 2 Intermolecular bonds for 3,6-diiodo-9-ethyl-9H-carbazole (Å and °)

| D–H...A | d(D–H) | d(H...A) | d(D...A) | <(DHA) |
|-------------------------------|--------|----------|----------|--------|
| C(5)–H(5)...I(1) ⁱ | 0.93 | 3.15 | 4.033(8) | 158.5 |

Symmetry transformations used to generate equivalent atoms

$$i = -x - 1, y - 0.5, -z$$

is only present for the C3 and C6 carbons directly bond to iodine atoms (Fig. 3). The significant errors with a root-mean-square deviation (RMS) of 6.23 ppm (for SO ZORA calculations RMS = 0.87 ppm) are visible for these two carbon chemical shifts predicted using non-relativistic calculations (Table 4). The RMS is smaller than for the previously studied 9-benzyl-3,6-diiodo-9H-carbazole [58]. The observed HALA effects are very close to earlier results for halogen-substituted carbon atoms [35, 41, 66] and for our previous study of benzylcarbazole derivative (there the HALA effect was –42 ppm) [58]. The other carbons, especially atoms responsible for the rigidity and planarity

Table 3 Comparison of selected geometric data (in Å) for 3,6-diiodo-9-ethyl-9H-carbazole (this work), 9-ethyl-9H-carbazole [62] and 3,6-diiodo-9H-carbazole [63] obtained from X-ray measurements at 293 K and non-relativistic calculations (NR B3LYP/6-311++G(3df,2pd)/6-311G**))

| Bond | Our results | | Literature | |
|-------------|-------------|--------|---|--|
| | X-ray | NR DFT | 9-Ethyl-9H-carbazole (X-ray) ^a | 3,6-Diiodo-9H-carbazole (X-ray) ^b |
| I(1)–C(3) | 2.101(8) | 2.135 | – | 2.096 (4) |
| I(2)–C(6) | 2.108(8) | 2.135 | – | 2.104 (3) |
| C(1)–C(9A) | 1.367(13) | 1.396 | 1.391(6) | 1.389 (5) |
| C(1)–C(2) | 1.377(13) | 1.391 | 1.365(6) | 1.366 (5) |
| C(2)–C(3) | 1.378(13) | 1.403 | 1.367(8) | 1.415 (5) |
| C(3)–C(4) | 1.379(12) | 1.389 | 1.374(6) | 1.376 (5) |
| C(4)–C(4A) | 1.393(12) | 1.398 | 1.385(6) | 1.391 (5) |
| C(4A)–C(9A) | 1.430(11) | 1.418 | 1.386(4) | 1.409 (5) |
| C(4A)–C(5A) | 1.442(11) | 1.446 | 1.437(9) | 1.445 (4) |
| C(5A)–C(8A) | 1.376(11) | 1.418 | – | 1.418 (5) |
| C(5A)–C(5) | 1.416(11) | 1.398 | – | 1.400 (4) |
| C(5)–C(6) | 1.365(12) | 1.389 | – | 1.373 (4) |
| C(6)–C(7) | 1.385(12) | 1.403 | – | 1.400 (5) |
| C(7)–C(8) | 1.395(13) | 1.391 | – | 1.378 (5) |
| C(8)–C(8A) | 1.372(12) | 1.396 | – | 1.387 (5) |
| C(8A)–N(9) | 1.405(10) | 1.388 | – | 1.375 (4) |
| N(9)–C(9A) | 1.380(11) | 1.388 | 1.372(8) | 1.378 (5) |
| N(9)–C(10) | 1.467(11) | 1.457 | – | – |
| C(10)–C(11) | 1.511(13) | 1.532 | – | – |
| RMS | | | | |
| C–C | | 0.021 | | 0.020 |
| C–N | | 0.012 | | 0.021 |
| C–I | | 0.031 | | 0.005 |
| Total | | 0.021 | | 0.019 |

^a Values taken from Ref. [62]^b Values taken from Ref. [63]

of the structure (C1, C8, C4, C5, C4A, C5A and C8A, C9A), also feel the presence of the heavy halogen atoms.

HOMA and NICS indexes

The calculated HOMA and NICS values are gathered in Table 5. HOMA indexes were calculated from Eq. (1) using $\alpha = 257.7$ and $R_{\text{opt}}(\text{CC}) = 1.388 \text{ \AA}$, $\alpha = 93.52$ and $R_{\text{opt}}(\text{CN}) = 1.344 \text{ \AA}$ [67] and bond lengths from B3LYP/6-311++G(3df,2pd) optimized geometries. For comparison, the corresponding HOMA values for benzene and pyrrole calculated at the same level of theory are 0.998 and 0.881, respectively. The calculated DFT HOMA indexes for pure 9H-carbazole are 0.958 for rings A and C and 0.690 for the five-membered B ring in carbazole molecule. The HOMA indexes are also compared with the 9H-carbazole values calculated by other authors. The most aromatic rings within the studied molecule are the two benzene rings labeled as A and C. For these rings the HOMA values are the same (0.944). The aromaticity of

Table 4 Comparison of experimental and theoretically predicted (non-relativistic and relativistic BHandHLYP/DZP) ¹³C NMR data for 3,6-diiodo-9-ethyl-9H-carbazole (in ppm)

| Atom numbering | Theoretical calculations | | Experimental data |
|----------------|--------------------------|---------|-------------------|
| | NR | SO ZORA | |
| C1=C8 | 121.41 | 110.12 | 110.65 |
| C2=C7 | 130.88 | 136.90 | 134.52 |
| C3=C6 | 125.97 | 85.92 | 81.67 |
| C4=C5 | 143.04 | 131.70 | 129.42 |
| C4A=C5A | 109.97 | 126.18 | 124.08 |
| C8A=C9A | 136.64 | 142.60 | 138.98 |
| C10 | 37.42 | 37.44 | 37.74 |
| C11 | 12.61 | 12.60 | 13.68 |
| RMS | 6.23 | 0.87 | |

these rings is smaller than in the unsubstituted 9H-carbazole molecule (HOMA = 0.958) calculated at the same level of theory. The least aromatic, both in our synthesized

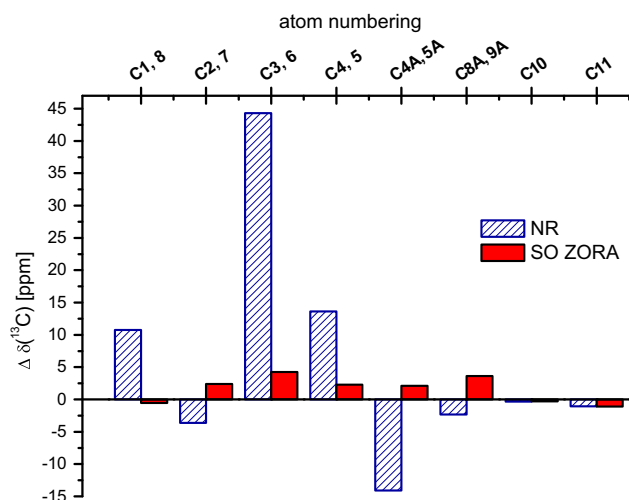


Fig. 3 Deviations of calculated from experimental chemical shifts ($\Delta\delta$) and the influence of relativistic effect on the accuracy of theoretically predicted carbon chemical shift ($\delta^{13}\text{C}$) for 3,6-diiodo-9-ethyl-9H-carbazole

compound and in 9H-carbazole, is the pyrrolic unit (ring B). In comparison with the pure pyrrole (HOMA = 0.881) and unsubstituted 9H-carbazole (HOMA = 0.679), the five-membered ring B is significantly less aromatic (HOMA = 0.661).

Table 5 also shows the three variants of NICS parameter [NICS(0), NICS(1) and NICS(1)_{zz}] for the studied carbazole derivative and for several related compounds. As a reference of aromaticity, the corresponding NICS values for benzene were calculated at B3LYP/6-311++G(3df,2pd) level of theory (−7.81, −10.21 and −29.88). The NICS values for all rings give the same results as HOMA indexes. The most aromatic rings are the benzene

units and less aromatic is the five-membered ring of 3,6-diiodo-9-ethyl-9H-carbazole. Due to the presence of two double bonds and nitrogen lone pair, the aromaticity of free pyrrole ring changes upon condensation with two benzene units. The fusion of aromatic rings affects the aromaticity of all units, and so the five-membered ring in carbazole molecule is less aromatic than in the free pyrrole. Analyzing the results, we observed that the most sensitive aromaticity index is the zz component of NICS(1). The data from Table 5 were recalculated and presented graphically in Fig. 4. In this case benzene was used as an arbitrary NICS reference for both six- and five-membered rings ($\text{NICS}_{\text{benzene}} - \text{NICS}_{\text{ring}}$). Figure 4 clearly shows that NICS(0) for benzene is less aromatic than for pyrrole, 9H-carbazole and our 3,6-diiodo-9-ethyl-9H-carbazole.

Conclusions

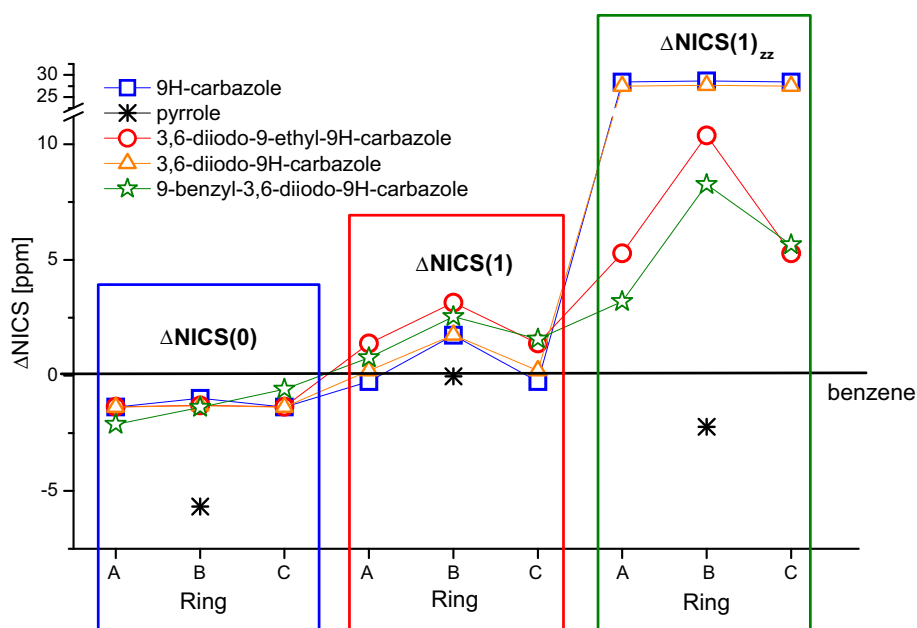
This paper reports on the crystal and molecular structure of 9-benzyl-3,6-diiodo-9H-carbazole. For the first time its crystal structure was determined at room temperature. A linear correlation between the experimental and the non-relativistic DFT calculated structural parameters was observed. We also reported on ^{13}C NMR parameters of the halogenated carbazole derivative. The ^{13}C NMR spectrum in CDCl_3 solution was measured. To accurately assign the observed ^{13}C NMR spectra it was important to employ the SO ZORA approach. Standard non-relativistic DFT calculations of the chemical shifts of atoms C3 and C6 for 3,6-diiodo-9-ethyl-9H-carbazole lead to significant errors (about −44 ppm). Finally, in this work we observed a linear correlation between theoretically predicted and

Table 5 Individual ring aromaticity indexes in 3,6-diiodo-9-ethyl-9H-carbazole, 9H-carbazole and in reference molecules (benzene, pyrrole)

| Compound | Ring | 3,6-Diiodo-9-ethyl-9H-carbazole | 9H-carbazole | | Reference molecules | |
|-----------------------|-------|---------------------------------|--------------|-------------------|---------------------|---------|
| | | | Calcul. | Lit. ^a | Benzene | Pyrrole |
| HOMA | A | 0.944 | 0.958 | 0.919 | 0.998 | 0.881 |
| | B | 0.661 | 0.690 | 0.679 | | |
| | C | 0.944 | 0.958 | 0.919 | | |
| | Total | 0.873 | 0.889 | – | | |
| NICS(0) | A | −9.16 | | −12.95 | −7.81 | −13.47 |
| | B | −9.10 | | −10.24 | | |
| | C | −9.16 | | −12.95 | | |
| NICS(1) | A | −8.83 | – | | −10.21 | −10.26 |
| | B | −7.06 | – | | | |
| | C | −8.83 | – | | | |
| NICS(1) _{zz} | A | −24.60 | – | – | −29.88 | −32.10 |
| | B | −19.50 | – | | | |
| | C | −24.60 | – | | | |

^a Values taken from Ref. [47]

Fig. 4 DFT calculated differences (Δ NICS) in aromatic indices for different rings of pyrrole, 9H-carbazole, 3,6-diiido-9H-carbazole, 3,6-diiido-9-ethyl-9H-carbazole and 9-benzyl-3,6-diiido-9H-carbazole (benzene was used as reference model for the Δ NICS indices)



experimental NMR parameters. Moreover, we estimated the changes in ring aromatic character via simple HOMA and NICS calculations. The most aromatic are the benzene units and less aromatic is the five-membered ring of 3,6-diiido-9-ethyl-9H-carbazole.

Acknowledgments K. Radula-Janik is recipient of a PhD fellowship from a project funded by the European Social Fund Stypendia doktoranckie-inwestycja w kadre naukową województwa opolskiego II. T. Kupka, K. Ejsmont and Z. Daszkiewicz were supported by the Faculty of Chemistry, University of Opole (Grants Number 8/WCH/2014-S, 7/WCH/2014-S and 1/WCH/2014-S). The calculation facilities and software in the Supercomputing and Networking Center ACK CYFRONET AGH in Krakow (Grant Number MNiSW/SGI3700/UOpolski/061/2008) and at the Supercomputing and Networking Center in Wrocław are also acknowledged. Stephan P.A. Sauer acknowledges support from DCSC and the Lundbeck foundation.

Open Access This article is distributed under the terms of the Creative Commons Attribution 4.0 International License (<http://creativecommons.org/licenses/by/4.0/>), which permits unrestricted use, distribution, and reproduction in any medium, provided you give appropriate credit to the original author(s) and the source, provide a link to the Creative Commons license, and indicate if changes were made.

References

- Grazulevicius JV, Strohriegl P, Pielichowski J, Pielichowski K (2003) Carbazole-containing polymers: synthesis, properties and applications. *Prog Polym Sci* 28:1297–1353
- Burroughes JH, Bradley DDC, Brown AR, Marks RN, MacKay K, Friend RH, Burn PL, Holmes AB (1990) Light-emitting diodes based on conjugated polymers. *Nature* 347:539–541
- Meerholz K, Volodin LB, Sandalphon Kippelen B, Peyghambarian N (1994) A photorefractive polymer with high optical gain and diffraction efficiency near 100%. *Nature* 71:497–500
- Wang Y (1996) Kirk–Othmer encyclopedia of chemical technology, vol 837, 4th edn. Wiley, New York, p 18
- Wang G, Qian S, Xu J, Wang W, Liu X, Lu X, Li F (2000) Enhanced photovoltaic response of PVK/C60 composite films. *Phys Part B* 279:116–119
- Boudreault PLT, Beaupré S, Leclerc M (2010) Polycarbazoles for plastic electronics. *Polym Chem* 1:127–136
- Beaupré S, Boudreault PLT, Leclerc M (2010) Solar-energy production and energy-efficient lighting: photovoltaic devices and white-light-emitting diodes using poly(2,7-fluorene), poly(2,7-carbazole), and poly(2,7-dibenzosilole) derivatives. *Adv Mater* 22:E6–E27
- Li J, Grimsdale AC (2010) Carbazole-based polymers for organic photovoltaic devices. *Chem Soc Rev* 39:2399–2410
- Morin J-F, Leclerc M (2002) 2,7-carbazole-based conjugated polymers for blue, green, and red light emission. *Macromolecules* 35:8413–8417
- Moerner WE, Silence SM (1994) Polymeric photorefractive materials. *Chem Rev* 94(1):127–155
- Zhang Y, Hokari H, Wada T, Shang Y, Marder SM, Sasabe H (1997) Synthesis of N-vinylcarbazole derivatives with acceptor groups. *Tetrahedron Lett* 38:8721–8722
- Grigalevicius S (2006) 3,6(2,7),9-Substituted carbazoles as electroactive amorphous materials for optoelectronics. *Synth Met* 156:1–12
- Hudson ZM, Wang Z, Helander MG, Lu ZH, Wang S (2012) N-Heterocyclic carbazole-based hosts for simplified single-layer phosphorescent OLEDs with high efficiencies. *Adv Mater* 24:2922–2928
- Zhang X, Wu Y, Ji S, Guo H, Song P, Han K, Wu W, Wu W, James TD, Zhao J (2010) Effect of the electron donor/acceptor orientation on the fluorescence transduction efficiency of the d-PET effect of carbazole-based fluorescent boronic acid sensors. *J Org Chem* 75:2578–2588
- Chen LX, Niu CG, Zeng GM, Huang GH, Shen GL, Yu RQ (2003) Carbazole as fluorescence carrier for preparation of doxycycline sensor. *Anal Sci* 19:295–298
- Curiel D, Cowley A, Beer PD (2005) Indolocarbazoles: a new family of anion sensors. *Chem Commun*. doi:10.1039/B412363H
- Zhang X, Chi L, Ji S, Wu Y, Song P, Han K, Guo H, James TD, Zhao J (2009) Rational design of d-PeT phenylethynylated-

- carbazole monoboronic acid fluorescent sensors for the selective detection of alpha-hydroxyl carboxylic acids and monosaccharides. *J Am Chem Soc* 131:17452–17463
18. Alkorta I, Elguero J (2010) Computational NMR spectroscopy, in computational spectroscopy: methods, experiments and applications, vol 2. Wiley-VCH Verlag GmbH & Co, KGaA, Weinheim
 19. Lampert H, Mikenda W, Karpfen A, Kaehlig H (1997) NMR shieldings in benzoyl and 2-hydroxybenzoyl compounds. *J Phys Chem A* 101:9610–9617
 20. Keeler J (2011) Understanding NMR spectroscopy, 2nd edn. Wiley, Chichester
 21. Berger S, Braun S (2004) 200 and more nmr experiments: a practical course. Wiley-VCH, Weinheim
 22. Jaroszewska-Manaj J, Maciejewska DIW (2000) Multinuclear NMR study and GIAO-CHF calculations of two quinoacridinium salts. *Magn Reson Chem* 38:482–485
 23. Barfield M, Fagerness P (1977) Density functional theory/GIAO studies of the ^{13}C , ^{15}N and ^1H NMR chemical shifts in aminopyrimidines and aminobenzenes: relationships to electron densities and amine group orientations. *J Am Chem Soc* 119:8699–8711
 24. Kupka T (2009) Convergence of H_2O , H_2 , HF , F_2 and F_2O nuclear magnetic shielding constants and indirect nuclear spin-spin coupling constants (SSCCs) using segmented contracted basis sets XZP, polarization-consistent pcS-n and pcJ-n basis sets and BHandH hybrid density functional. *Magn Reson Chem* 47:959–970
 25. Kupka T, Stachów M, Nieradka M, Kaminsky J, Pluta T (2010) Convergence of nuclear magnetic shieldings in the Kohn–Sham limit for several small molecules. *J Chem Theory Comput* 6:1580–1589
 26. Wolinski K, Hilton JF, Pulay P (1990) Efficient implementation of the gauge-independent atomic orbital method for NMR chemical shift calculations. *J Am Chem Soc* 112:8251–8260
 27. Lee C, Yang W, Parr RG (1988) Development of the Colle-Salvetti correlation-energy formula into a functional of the electron density. *Phys Rev B* 37(2):785–789
 28. Becke AD (1988) Density-functional exchange-energy approximation with correct asymptotic behavior. *Phys Rev A* 38:3098–3100
 29. Becke AD (1993) A new mixing of Hartree-Fock and local density-functional theories. *J Chem Phys* 98:1372–1377
 30. Erra-Balsells R (1988) ^{13}C NMR spectra of substituted carbazoles and azacarbazoles (b-carbolines). *Magn Reson Chem* 26:1109–1112
 31. Al-Sultani KTA (2010) Synthesis and evaluation of the biological activity for some carbazole derivatives. *J Al-Nahrain Univ* 13:31–38
 32. Claramunt RM, Cornago P, Sanz D, Santa-María D, Foces-Foces C, Alkorta I, Elguero J (2002) 1-Benzoylazoles: an experimental (NMR and crystallography) and theoretical study. *J Mol Struct* 605:199–212
 33. Kupka T, Pasterna G, Jaworska M, Karali A, Dais P (2000) GIAO NMR calculations for carbazole, and its *N*-methyl and *N*-ethyl derivatives. comparison of theoretical and experimental ^{13}C chemical shifts. *Magn Reson Chem* 38:149–155
 34. Pyykkö P, Görling A, Rösch N (1987) A transparent interpretation of the relativistic contribution to the NMR ‘heavy atom chemical shift’. *Mol Phys* 61:195–205
 35. Malkina OL, Schimmelpennig B, Kaupp M, Hess BA, Chandra P, Wahlgren U, Malkin VG (1998) Spin-orbit corrections to NMR shielding constants from density functional theory. How important are the two-electron terms? *Chem Phys Lett* 296:93–104
 36. Komorovský S, Repiský M, Malkina OL, Malkin VG (2010) Fully relativistic calculations of NMR shielding tensors using restricted magnetically balanced basis and gauge including atomic orbitals. *J Chem Phys* 132:154101
 37. Autschbach J, Ziegler T (2002) Relativistic computation of NMR shieldings and spin-spin coupling constants. *Encyclopedia of nuclear magnetic resonance*, vol 9. Wiley, Chichester
 38. Kaupp M, Malkin VG, Malkina OL, Salahub DR (1995) Calculation of ligand NMR-chemical shifts in transition-metal complexes using ab initio effective-core potentials and density functional theory. *Chem Phys Lett* 235:382–388
 39. Kaupp M, Malkina OL (1998) Ab initio ECP/DFT analysis of ^{13}C and ^1H chemical shifts and bonding in mercurimethanes and organomercury hydrides: the role of scalar relativistic. *J Chem Phys* 108:3648–3659
 40. Kaupp M (1996) NMR chemical-shift anomaly and bonding in piano-stool carbonyl and related complexes. An ab initio ECP/DFT study. *Chem Eur J* 2:348–358
 41. Wodyński A, Gryff-Keller A, Pecul M (2013) The influence of a presence of a heavy atom on ^{13}C shielding constants in organomercury compounds and halogen derivatives. *J Chem Theory Comput* 9:1909–1917
 42. Chang C, Pelissier M, Durand P (1986) Regular two-component pauli-like effective Hamiltonians in dirac theory. *Phys Scr* 34:394–404
 43. Van Lenthe E, Baerends EJ, Snijders JG (1993) Relativistic regular two-component Hamiltonians. *J Chem Phys* 99:4597–4610
 44. Wolff SK, Ziegler T, van Lenthe E, Baerends EJ (1999) Density functional calculations of nuclear magnetic shieldings using the zeroth-order regular approximation (ZORA) for relativistic effects: ZORA nuclear magnetic resonance. *J Chem Phys* 110:7689–7698
 45. Russo TV, Martin RL, Hay PJ (1995) Effective core potentials for DFT calculations. *J Phys Chem* 99(47):17085–17087
 46. Wodyński A, Pecul M (2014) The influence of a presence of a heavy atom on the spin-spin coupling constants between two light nuclei in organometallic compounds and halogen derivatives. *J Chem Phys* 140(2):024319. doi:10.1063/1.4858466
 47. Poater J, García-Cruz I, Illas F, Solà M (2004) Discrepancy between common local aromaticity measures in a series of carbazole derivatives. *Phys Chem Chem Phys* 6:314–318
 48. Kruszewski J, Krygowski TM (1972) Definition of aromaticity basing on the harmonic oscillator model. *Tetrahedron Lett* 13(36):3839–3842
 49. Krygowski TM (1993) Crystallographic studies of inter- and intramolecular interactions reflected in aromatic character of π -electron systems. *J Chem Inf Comput Sci* 33:70–78
 50. Krygowski TM, Szatyłowicz H, Stasyuk OA, Dominikowska J, Palusiak M (2014) Aromaticity from the viewpoint of molecular geometry: application to planar systems. *Chem Rev* 114:6383–6422
 51. PvR Schleyer, Maerker C, Dransfield A, Jiao H, van Eikema Hommes NJR (1996) Nucleus-independent chemical shifts: a simple and efficient aromaticity probe. *J Am Chem Soc* 118:6317–6318
 52. Chen Z, Wannere CS, Corminboeuf C, Puchta R, PvR Schleyer (2005) Nucleus-independent chemical shifts (NICS) as an aromaticity criterion. *Chem Rev* 105:3842–3888
 53. Chuang CN, Chuang H-J, Wang Y-X, Chen S-H, Huang J-J, Leung M-K, Hien K-H (2012) Polymers with alkyl main chain pendent biphenyl carbazole or triphenylamine unit as host for polymer light emitting diodes. *Polimer* 53:4983–4992
 54. Oxford Diffraction: CrysAlis CCD and CrysAlis RED (2008) Versions 1.171.32.29 edn. Oxford Diffraction Ltd, Abingdon
 55. Sheldrick GM (2008) A short history of SHELX. *Acta Cryst A* 64:112–122
 56. Cambridge Crystallographic Data Centre (CCDC) 12 Union road C, CB21EZ, UK

57. Frisch MJ, Trucks GW, Schlegel HB, Scuseria GE, Robb MA, Cheeseman JR, Scalmani G, Barone V, Mennucci B, Petersson GA, Nakatsuji H, Caricato M, Li X, Hratchian HP, Izmaylov AF, Bloino J, Zheng G, Sonnenberg JL, Hada M, Ehara M, Toyota K, Fukuda R, Hasegawa J, Ishida M, Nakajima T, Honda Y, Kitao O, Nakai H, Vreven T, Montgomery JA, Peralta JE, Ogliaro F, Bearpark M, Heyd JJ, Brothers E, Kudin KN, Staroverov VN, Kobayashi R, Normand J, Raghavachari K, Rendell A, Burant JC, Iyengar SS, Tomasi J, Cossi M, Rega N, Millam JM, Klene M, Knox JE, Cross JB, Bakken V, Adamo C, Jaramillo J, Gomperts R, Stratmann RE, Yazyev O, Austin AJ, Cammi R, Pomelli C, Ochterski JW, Martin RL, Morokuma K, Zakrzewski VG, Voth GA, Salvador P, Dannenberg JJ, Dapprich S, Daniels AD, Farkas O, Foresman JB, Ortiz JV, Cioslowski J, Fox DJ (2009) Gaussian 09, revision A.02. Gaussian Inc., Wallingford
58. Radula-Janik K, Kupka T, Ejsmont K, Daszkiewicz Z, Sauer SPA (2015) Molecular modeling and experimental studies on structure and NMR parameters of 9-benzyl-3,6-diiido-9H-carbazole. *Struct Chem* 26:997–1006
59. Versluis L, Ziegler T (1988) The determination of molecular structures by density functional theory. The evaluation of analytical energy gradients by numerical integration. *J Chem Phys* 88:322–328
60. ADF2012 S (2012) Theoretical chemistry, Vrije Universiteit, Amsterdam, The Netherlands. <http://www.scm.com>
61. Belskii VK (1985) Structure of carbazole. *Kristallografiya* 30:193–194
62. Kimura T, Kai Y, Yasuoka N, Kasai N (1985) The crystal and molecular structure of N-ethylcarbazole. *Bull Chem Soc Jpn* 58(8):2268–2271
63. Xie Y-Z, Jin J-Y, Jin G-D (2012) 3,6-Diiido-9H-carbazole. *Acta Cryst E* 68:o1242. doi:10.1107/S1600536812012901
64. Jeffrey GA (1997) An introduction to hydrogen bonding. Oxford University Press, Oxford
65. Bondi A (1964) Van der Waals volumes and radii. *J Phys Chem* 68:441–451
66. Radula-Janik K, Kupka T, Ejsmont K, Daszkiewicz Z, Sauer SPA (2013) Halogen effect on structure and ¹³C NMR chemical shift of 3,6-disubstituted-N-alkyl carbazoles. *Magn Reson Chem* 51:630–635
67. Krygowski TM, Cyrański MK (2001) Structural aspects of aromaticity. *Chem Rev* 101:1385–1420